ORIGINAL STUDY

Potential field data interpretation to detect the parameters of buried geometries by applying a nonlinear least-squares approach

Khalid S. Essa[2] · **Eid. R. Abo-Ezz[1]**

Abstract
The detection of buried geometrical model parameters is vital to full interpretation of potential field data, especially that related to gravity and/or self-potential anomalies. This study introduced a proposed non-linear least-squares algorithm for solving a combined formula for gravity and self-potential anomalies due to simple geometric shapes. This proposed algorithm was relied upon delimiting the origin anomaly value and two symmetric anomaly values with their equivalent distances along with the anomaly profile in order to invert the buried geometry model parameters. After that, a root mean square error (μ-value) for each parameter value at different postulated shape factor was assessed. The μ-value was considered as a benchmark for detecting the true-values of the subsurface geometry structures. The efficacy and rationality of the proposed approach were revealed by numerous synthetic cases with and without random noise. Furthermore, the sensitivity analysis between shape factor and μ-value were investigated on synthetic gravity and self-potential data. It was evident that the inverted parameters were reliable with the genuine ones. This proposed method was tested on samples of gravity data and self-potential data taken from Senegal and USA. To judge the satisfaction of this approach, the results gained were compared with other available geological or geophysical information in the published literature.

Keywords The least-squares algorithm · The root-mean squared errors · Model parameters · Mineral exploration

✉ Khalid S. Essa
essa@sci.cu.edu.eg

✉ Eid. R. Abo-Ezz
e.aboezz@psau.edu.sa

1   Department of Physics, College of Science and Humanities, Prince Sattam Bin Abdulaziz University, Al-Kharj 11942, Saudi Arabia

2   Geophysics Department, Faculty of Science, Cairo University, P.O. 12613, Giza, Egypt

1 Introduction

The geometrical parameters due to the causative source bodies are a commonly requested task in the interpretation of geophysical data. Many methods are derived to accomplish this task. For instance, a combined gravity or self-potential anomaly formula produced for simple geometrically shaped models can be signified through an analytical formula. This formula is a useful component to determine the depth, shape factor, polarization angle and amplitude factor connected to the physical effects of a buried structure. In this method, the gravity inversion aims to estimate the depth, amplitude and shape factors, while the self-potential inversion aims to estimate the same mentioned parameters and one or more parameters, which is called the angle of polarization for simple geometric shaped structures. These geometric shapes include a sphere, a horizontal cylinder, a semi-infinite vertical cylinder, and a dike. This method is reasonably suitable in some conditions, where some geological situations can have a distinct gravity or self-potential anomaly, which can be inverted as a single model. This suggests that quick and truthful quantitative elucidation approaches rely on simple geometric anomalies utilized for defining the inverse parameters of the subsurface model structures from observed gravity and self-potential data.

A number of fixed geometrical methods were introduced to decide the subsurface structure model parameters from gravity or self-potential data. They depend on graphical approaches, which apply characteristic points and distances (Nettleton 1976; Ram Babu and Atchuta Rao 1988; Essa 2007a), using matching curves (Murthy and Haricharan 1984) and using nomograms (Paul 1965; Bhattacharya and Roy 1981) all of them involving many approximations.

Several numerical methods have been established to construe gravity or self-potential data which includes Fourier transformation method (Sharma and Geldart 1968; Roy and Mohan 1984; Asfahani et al. 2001), Ratio methods (Bowin et al. 1986), Euler deconvolution (Thompson 1982; Reid et al. 1990; Roy et al. 2000), Werner deconvolution (Hartmann et al. 1971; Jain 1976), Mellin transformation (Mohan et al. 1986; Babu et al. 1991), Walsh transformation technique (Shaw et al. 1998; Al-Garni 2008), analytic signal method (Nandi et al. 1997; Sundarajan et al. 1998), linear and non-linear least-squares (Gupta 1983; Abdelrahman et al. 2003, 2008; El-Araby 2004; Essa et al. 2008), neural network application (Osman et al. 2007; Al-Garni 2010; Hajian et al. 2012), gradients (Aboud et al. 2004; Essa 2007b; Essa and Elhussein 2017; Roy 2019), and moving average method (Abdelrahman et al. 2006a, and 2009), 2D and 3D tomography and inversion (Biswas and Sharma 2017; Pham et al. 2018; Oksum et al. 2019; Vasiljević et al. 2019). The results of these approaches require a density data for the gravity elucidation and an existing intensity and a resistivity data for the self-potential explanation as a feature of the input, alongside a similar depth information gained from geologic as well as other geophysical information. Consequently, the subsequent model can fluctuate broadly relying upon these components if the gravity and self-potential inverse problem are ill-posed, unstable, and non-unique (Tarantola 2005; Mehanee and Essa 2015). Typical methods for acquiring steady solutions of an ill-posed inverse problem incorporate some regularization approaches (Tikhonov and Arsenin 1977; Ghanati et al. 2017). The three-dimensional gravity and self-potential result rely on a rigorous, estimation time, and priori information for inverting the model parameters. In addition, metaheuristic algorithms such as particle swarm algorithm (Essa and Munschy 2019; Essa 2020), anti-colony algorithm (Srivastava et al. 2014), simulated annealing (Biswas 2016a , b), and genetic algorithm (Montesinos et al. 2005; Di Maio et al. 2016) can be proposed to infer gravity and self-potential anomalies.

Moreover, Essa (2011) developed a semi-automatic approach to interpret gravity and self-potential data using a combined formula for both anomalies, which depends on knowing known the shape of the buried structures to estimate the depth and other model parameters.

The main objective and goal of the study is to develop a well-organized inversion method to overcome ill-posed and non-unique interpretation of gravity and self-potential data. The proposed nonlinear least-squares approach for gravity or self-potential inversion was established to estimate the depth (z) of the subsurface structures. The inverted problem of the depth was transformed into a nonlinear formula as $z = f(z)$. This formula was deciphered for the depth by minimizing the objective function. By means of such assessed depth, a polarization angle and an amplitude factor emerged from the measured gravity or self-potential. The proposed approach relied on appraising the root mean square (μ-value) of the calculated buried model parameters for the causative bodies, which was utilized as a typical for detecting the optimal fit parameters of the subsurface model structure.

Finally, a nonlinear least-squares algorithm was applied to the synthetic examples with and without random noise. In addition, gravity and self-potential data set were used to investigate the sensitivity analysis of this method. This method was simultaneously tested on two real data sets, which revealed that the detected depths and other model parameters were in respectable covenant with the real ones.

1.1 The methodology

Essa (2010) proposed a combined gravity and/or self-potential for the simple shaped geological structures (spheres, cylinders, and sheets) as follows:

$$g(x_i,\ z) = A\frac{z^j}{\left(x_i^2 + z^2\right)^q}, \tag{i}$$

$$V(x_i,\ z) = A\frac{x_i(\cos\theta) + z(\sin\theta)}{\left(x_i^2 + z^2\right)^q}, \tag{ii}$$

to produce the following form:

$$P(x_i,\ z) = A\frac{cx_i(\cos\theta)^n + z^j(\sin\theta)^m}{\left(x_i^2 + z^2\right)^q},\ i = 0,\ \pm 1,\ \pm 2,\ \pm 3, \ldots, \pm k \tag{1}$$

where z is the depth of the body (unit), θ is the polarization angle (in case of self-potential data only), A is an amplitude factor depending on the physical features of the model (in gravity: mGal×unit^{2q-j} but in self-potential mV×unit^{2q-j}), x_i is the horizontal coordinates (unit) and q is the shape factor of the model. Values of c, m, n, j, and q are specified in Table 1.

Equation (1) gives the next formula at the location of the anomaly origin, i.e. $x_i = 0$ and $P(x_i, z) = P(0)$

$$A = \frac{P(0)z^{2q-j}}{(\sin\theta)^m}, \tag{2}$$

From Eq. (1), the next equations are attained at $x_i = \pm N$, $N = 1, 2, 3, \ldots, k$

Table 1 Values of the parameters c, m, n, and j for various simple-geometric shapes in case of gravity and self-potential approaches (Essa, 2011)

Shape	Gravity				Self-potential			
	c	m	n	j	c	m	n	j
Semi-infinite vertical cylinder (q=0.5)	0	0	0	0	1	1	1	1
Horizontal cylinder (q=1.0)	0	0	0	1	1	1	1	1
Sphere (q=1.5)	0	0	0	1	1	1	1	1
Finite vertical cylinder (q=1.0)	0	0	0	1	1	1	1	1
A horizontal sheet (q=0.0)	0	0	0	0	1	1	1	1

$$P(+N) = A\frac{cN(\cos\theta)^n + z^j(\sin\theta)^m}{\left(N^2 + z^2\right)^q}, \quad x_i = +N \tag{3}$$

and

$$P(-N) = A\frac{-cN(\cos\theta)^n + z^j(\sin\theta)^m}{\left(N^2 + z^2\right)^q}, \quad x_i = -N \tag{4}$$

From Eqs. (3) and (4), new two variables F and T are introduced as follows:

$$F = \frac{P(+N) + P(-N)}{2P(0)}, \tag{5}$$

and

$$T = \frac{P(+N) - P(-N)}{2P(0)}. \tag{6}$$

From applying Eq. (5), the next form in shape (q) is deduced

$$q = \frac{lnF}{ln\left(\frac{z^2}{N^2+z^2}\right)}. \tag{7}$$

By using Eq. (3) and (4) and relieving in Eq. (6), we obtain the next form:

$$\frac{(\cos\theta)^n}{(\sin\theta)^m} = \frac{T\left(N^2 + z^2\right)^q}{cNz^{2q-j}}. \tag{8}$$

In this way, we can rewrite Eq. (1) employing Eqs. (7) and (8) as follows

$$P(x_i, z) = P(0)W(x_i, z), \tag{9}$$

where

$$W(x_i, z) = \frac{2x_i T\left(N^2 + z^2\right)^{lnF/ln\left(\frac{z^2}{N^2+z^2}\right)} + 2Nz^{lnF/ln\left(\frac{z^2}{N^2+z^2}\right)}}{2N\left(x_i^2 + z^2\right)^{lnF/ln\left(\frac{z^2}{N^2+z^2}\right)}}.$$

The unidentified depth in Eq. (9) can be gained applying the least-squares sense by minimizing the subsequent mathematical objective function in the real space. The form is:

$$z = arg \min \varphi(z) = \sum_{i=1}^{k} [\varphi(z)]^2 = \sum_{i=1}^{k} \left[P(x_i) - P(0)W(x_i, z) \right]^2 = minmum. \quad (10)$$

where $P(x_i)$ is the observed gravity or self-potential anomaly at x_i, $P(0)$ is the anomaly value at the origin ($x_i = 0$), and k is the total number of collected data.

So, Eq. (10) can be solved using minimization, i.e., $\frac{\partial \sum_{i=1}^{k} [P(x_i) - P(0)W(x_i,z)]^2}{\partial z} = 0$, which leads to the next nonlinear formula in z:

$$f(z) = \sum_{i=1}^{k} \left[P(x_i) - P(0)W(x_i, z) \right] W^*(x_i, z) = 0, \quad (11)$$

where

$$W^*(x_i, z) = \frac{\partial W(x_i, z)}{\partial z}.$$

Hence, Eq. (11) finally is

$$z_f = \frac{\sum_{i=1}^{k} P(0)W^*(x_i, z_i)}{P(0) \sum_{i=1}^{k} W(x_i, z_i) W^*(x_i, z_i)} \quad (12)$$

The depth (z) can be obtained by solving the nonlinear Eq. (12) applying a suitable iteration method (Mustoe and Barry 1998). The iteration form of Eq. (12) is:

$$z_f = f(z_i), \quad (13)$$

where z_f and z_i are the final and the initial depths, the iterative procedure finished at $\left| z_f - z_i \right| \leq E$, where E is a real number nearby zero. So, any initial guessing for the depth affected well because there is only one global minimum, i.e., no restrictions for the optimum range for the initial guess required.

Finally knowing the depth value, the shape factor (q), the angle of polarization (only in case of self-potential data) and the amplitude factor values are obtained from Eqs. (7), (8), and (2), respectively.

1.2 Determination of the best-fit parameters

The root mean square error (µ-value) has been utilized as a standard statistical metric to detect the model performance in the field of geosciences (Chai and Draxler 2014), i.e., the average model prediction error in the model parameters of interest.

Using the estimated model parameters from gravity or self-potential anomalies, we compute the µ-value in the following form:

$$\mu - value = \sqrt{\frac{\sum_{i=-k}^{+k} \left[P(x_i) - P(x_i, z) \right]^2}{2k + 1}}, \quad (14)$$

where $2k+1$ is the number of collected points, and $P(x_i)$ and $P(x_i, z)$ are individually the observed and the computed forward model of gravity or self-potential anomalies. The model parameters, which give the minimum μ-values are the optimal fit parameters. In this way, we can detect the best-fit source parameters outcomes from all gravity or self-potential data.

Hence, we recommend a statement of origin to delineate data. In practice, since a field traverse has a subjective origin, the place of the model ($x_i = 0$) in Eq. (1) must be delineated. In the gravity method, the maxima and/or the minima values of the profiles can be considered as the place of the origin of the body ($x_i = 0$). While, the straight line connecting the maxima to the minima of the self-potential anomaly profile intersects the anomaly curve at the point $x_i = 0$ (Stanley 1977). In addition, Abdelrahman et al. (2006b) acquainted a semi-automatic approach to describe the horizontal position of the structure applying a least-squares sense from a self-potential residual anomaly.

1.3 Synthetic examples

The benefits of the proposed method in this study were inspected through different synthetic cases, which include noise and anomalies produced by simple geometrically shapes (e.g., semi-infinite vertical, cylindrical, horizontal cylindrical, and spherical). The anomalies of the relevant models were generated using Eq. (1). In all cases studied, the synthetic anomalies were computed along with a profile extending 40 units with an interval of 1 unit.

1.4 First synthetic case (gravity anomalies)

Three gravity anomalies due to an infinitely extended semi-infinite vertical cylinder, horizontal cylinder, and sphere with source parameters: A = 500 mGal × unit, z = 3 unit and q = 0.5, A = 1500 mGal × unit, z = 5 unit and q = 1.0, and A = 2500 mGal × unit^2, z = 7 unit and q = 1.5 were considered. The gravity anomalies of these three models are shown in Fig. 1. The generated gravity anomalies are inferred applying the procedures of the proposed approach, i.e., for each N value, the buried model parameters (z, q, A) was computed by utilizing Eqs. (12), (7), and (2), respectively. Besides, the fit between the observed and computed gravity anomaly was computed using the μ-value for each set of solutions through applying Eq. (14), whereas the evaluated gravity source parameters are presented in Tables 2, 3, and 4. The results in Tables 2, 3, and 4 demonstrate that the error (e) in all estimated parameters and the μ-value is equal to zero in case of free-noise anomalies used.

To check the stability of the suggested approach in the occurrence of noisy data, each gravity anomaly, P(xi), was tainted with a 10% random noise. The contaminated gravity anomalies were inferred by using the proposed method as mentioned above. The results are given in Tables 2, 3, and 4 for the same N value as follows:

First, Table 2 (in case of estimating parameters for the semi-infinite vertical cylinder) shows the estimated values for each model parameter (z, q, A), their percentage of error (e), and the μ-value. The minimum μ-value (5.80 mGal) happens at the N value equal 2 unit and the value of the depth (z) is 2.92 unit with 2.67% error, the shape (q) is 0.49 with 2% error, and the amplitude factor (A) equals 485.86 mGal × unit with 2.83% error.

Second, Table 3 for the horizontal cylinder model displays the values of all estimated parameters as z = 5.21 unit, q = 1.02, and A = 1575.18 mGal × unit, and the error in each parameter is 4.2%, 2%, and 5.01%, respectively. This result happens at the minimum μ-value (7.32 mGal) at N = 3 unit.

Table 2 Numerical results of the present method applied to synthetic example; the gravity anomaly profile over a semi-infinite vertical cylinder model (q=0.5) with model parameters are z=3 unit, A=500 mGal×unit, and profile length=40 unit without and with a 10% random noise

Synthetic data without random noise

N (unit)	z (unit)	e (%)	q (dimensionless)	e (%)	A (mGal×unit)	e (%)	μ-value (mGal)
2	3	0	0.5	0	500	0	0
3	3	0	0.5	0	500	0	0
4	3	0	0.5	0	500	0	0
5	3	0	0.5	0	500	0	0
6	3	0	0.5	0	500	0	0
7	3	0	0.5	0	500	0	0
8	3	0	0.5	0	500	0	0
9	3	0	0.5	0	500	0	0
10	3	0	0.5	0	500	0	0

Synthetic data with a 10% random noise

N (unit)	z (unit)	e (%)	q (dimensionless)	e (%)	A (mGal×unit)	e (%)	μ-value (mGal)
2	2.92	2.67	0.49	2.00	485.86	2.83	5.80
3	2.85	5.00	0.47	6.00	469.18	6.16	7.654
4	2.94	2.00	0.49	2.00	491.82	1.64	8.73
5	3.01	0.33	0.51	2.00	508.36	1.67	10.09
6	2.88	4.00	0.48	4.00	479.21	4.16	10.91
7	2.92	2.67	0.49	2.00	486.79	2.64	11.64
8	3.03	1.00	0.51	2.00	507.96	1.59	12.61
9	2.90	3.33	0.48	4.00	482.91	3.41	13.24
10	2.85	5.00	0.47	6.00	474.12	5.17	13.91

Finally, Table 4 clearly indicates that μ-value (0.68 mGal at N=2 unit) is the minima value at which the values of depth (6.86 unit), the shape (1.51), and the amplitude factor (2542.49 mGal×unit^2) and their errors are 2%, 0.67%, and 1.69%, respectively.

1.5 Second synthetic case (self-potential anomalies)

Using Eq. (1), three synthetic self-potential anomalies for a thin sheet, a horizontal cylinder, and a spherical model were created. The source parameters of these self-potential anomalies were: A=−500 mV, z=2 unit, θ=30° and q=0.5, A=−2000 mV×unit, z=4 unit, θ=50° and q=1.0, and A=−3500 mV×unit^2, z=6 unit, θ=70° and q=1.5 (Fig. 2). The generated self-potential anomalies can be interpreted by using the proposed approach. For every N value, the model parameters (z, θ, q, and A) are computed by utilizing Eqs. (12), (8), (7), and (2), respectively. The μ-value is also computed applying Eq. (14) to measure the optimal fit between the observed and computed self-potential anomalies (Tables 5, 6, and 7).

In case of using these anomalies without adding any noise, the results of the estimated parameters in Tables 5, 6, and 7 demonstrate that the error (e) in each parameter and the

Table 3 Numerical results of the present method applied to synthetic example; the gravity anomaly profile over a horizontal cylinder model (q=1.0) with model parameters are z=5 unit, A=1500 mGal×unit, and profile length=40 unit without and with a 10% random noise

Synthetic data without random noise

N (unit)	z (unit)	e (%)	q (dimensionless)	e (%)	A (mGal×unit)	e (%)	μ-value (mGal)
2	5	0	1	0	1500	0	0
3	5	0	1	0	1500	0	0
4	5	0	1	0	1500	0	0
5	5	0	1	0	1500	0	0
6	5	0	1	0	1500	0	0
7	5	0	1	0	1500	0	0
8	5	0	1	0	1500	0	0
9	5	0	1	0	1500	0	0
10	5	0	1	0	1500	0	0

Synthetic data with a 10% random noise

N (unit)	z (unit)	e (%)	q (dimensionless)	e (%)	A (mGal×unit)	e (%)	μ-value (mGal)
2	4.96	0.8	1.00	0	1488.21	0.79	9.12
3	5.21	4.20	1.02	2.00	1575.18	5.01	7.32
4	5.28	5.60	1.04	4.00	1734.00	15.60	8.43
5	5.14	2.80	0.99	1.00	1461.47	2.57	9.47
6	5.28	5.60	1.04	4.00	1732.79	15.52	10.35
7	5.20	4.00	1.02	2.00	1572.26	4.82	11.18
8	5.20	4.00	1.02	2.00	1579.09	5.27	11.94
9	5.16	3.20	1.00	0	1504.56	0.30	12.67
10	5.22	4.40	1.02	2.00	1619.79	7.99	13.35

μ-value are equal to zero. While in case of adding a 10% random noise, the inversion process run and the optimal fit parameters are picked at the minimum μ-value as follows:

Table 5 shows that the minima μ-value is 10.78 mV occurring at N=3 unit and at which the optimal fit parameters (z, θ, q, and A) are 2.08 unit, 28.98°, 0.52, −496.75 mV with error of 4%, 3.40%, 3.37%, 0.65%, respectively. Table 6 further displays the results for the horizontal cylinder model self-potential inversion where the minima μ-value is 6.26 mV occurring at N=10 unit and at which the optimal fit parameters (z, θ, q, and A) are 3.85 unit with 3.75% error, 50.98° with error of 1.96%, 0.98 with 2.47%, and −1970.04 mV×unit with 1.50% error, respectively. Moreover, Table 7 presents the inverted parameter values (z, θ, q, and A) for a spherical model with values as 6.19 unit, 69.47°, 1.5, and −3553.26 mV×unit² , with percentage of errors of 3.17%, 0.76%, 0%, and 1.52%, respectively, when this happens at N=9 unit with the lowest μ-value (8.09 mV).

1.6 Third synthetic case (the effect of the location of origin)

To examine the effect of the location of origin; two synthetic data models with and without random errors were selected. The gravity model with the parameters: A=600 mGal×unit,

Table 4 Numerical results of the present method applied to synthetic example; the gravity anomaly profile over a sphere model (q = 1.5) with model parameters are z = 7 unit, A = 2500 mGal × unit^2, and profile length = 40 unit, without and with a 10% random noise

Synthetic data without random noise

N (unit)	z (unit)	e (%)	q (dimensionless)	e (%)	A (mGal × unit^2)	e (%)	μ-value (mGal)
2	7	0	1.5	0	2500	0	0
3	7	0	1.5	0	2500	0	0
4	7	0	1.5	0	2500	0	0
5	7	0	1.5	0	2500	0	0
6	7	0	1.5	0	2500	0	0
7	7	0	1.5	0	2500	0	0
8	7	0	1.5	0	2500	0	0
9	7	0	1.5	0	2500	0	0
10	7	0	1.5	0	2500	0	0

Synthetic data with a 10% random noise

N (unit)	z (unit)	e (%)	q (dimensionless)	e (%)	A (mGal × unit^2)	e (%)	μ-value (mGal)
2	6.86	2.00	1.51	0.67	2542.49	1.69	0.68
3	7.04	0.57	1.50	0	2427.14	2.91	0.75
4	6.83	2.42	1.49	0.67	2318.32	7.27	1.36
5	7.06	0.86	1.51	0.67	2576.28	3.05	1.06
6	6.81	2.71	1.48	1.33	2204.45	11.82	1.66
7	6.83	2.43	1.49	0.67	2263.19	9.47	2.13
8	6.84	2.28	1.49	0.67	2351.55	5.93	2.52
9	7.02	0.28	1.49	0.67	2362.36	5.51	1.50
10	7.01	0.14	1.49	0.67	2343.77	6.25	1.59

z = 8 unit, and q = 1.0, and a self-potential model with A = 600 mV × unit, z = 8 unit, θ = 30° and q = 1.0 investigated the effect of changing the value of location of origin by introducing an error of ± 0.5, ± 1.0, ± 1.5, and ± 2.5 unit to the location of origin in Eq. (1) (Fig. 3). Figure 3 shows the significance of choosing the location of origin in all the different model calculations vis-à-vis their μ-value errors.

In synthetic data without random errors, Fig. 3a, b show that the μ-value decreases to reach zero value at the correct solutions. But in synthetic data with a 10% random error, Fig. 3a, b show that the μ-value has a minimum value at the correct solutions. This kind of sensitivity analysis is important and necessary to test the effect of the location of origin as an important parameter in calculations.

1.7 Field examples

To clarify the benign application of new approaches established in the earlier sections, two residual field anomalies from Senegal and USA were sampled to interpret and inspect the stability and validity of the proposed method.
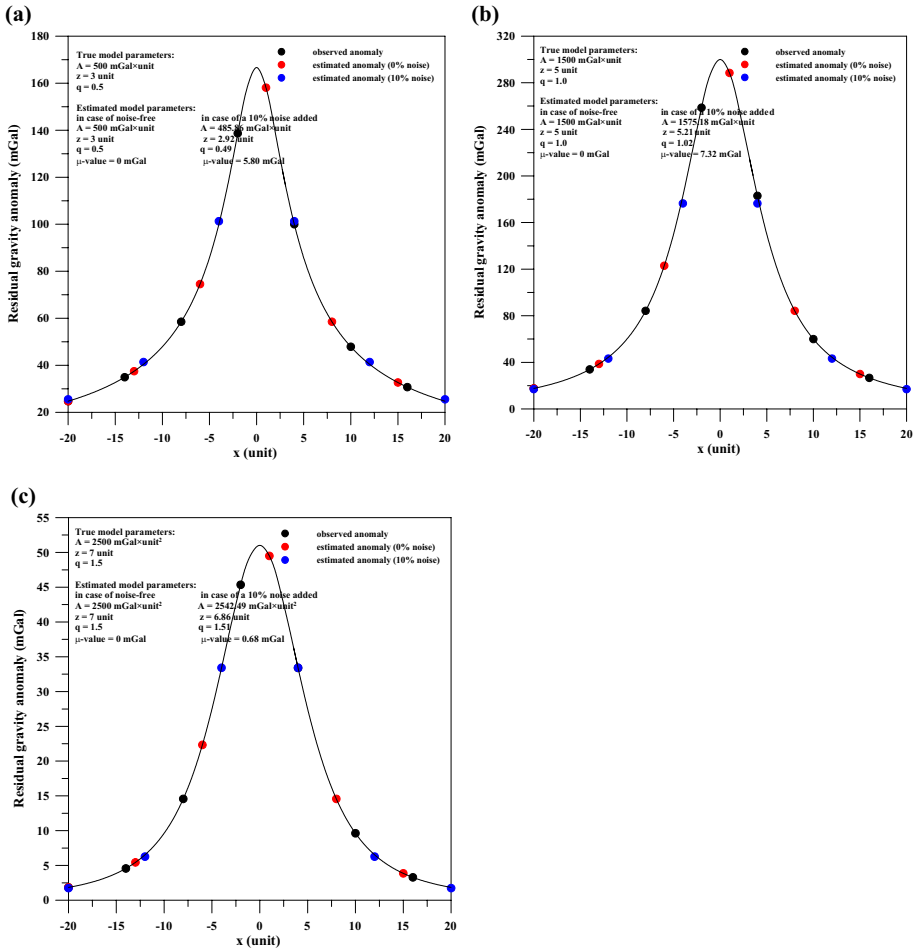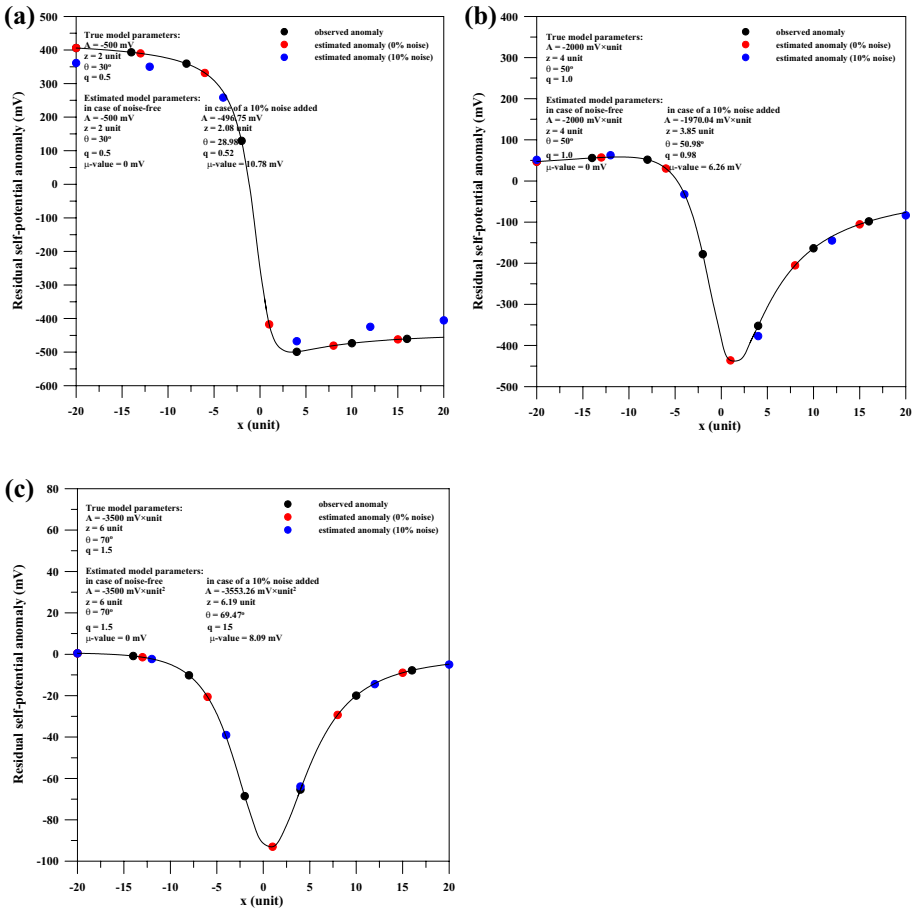
Fig. 1 The residual gravity anomalies of the buried structures representing by: **a** a semi-infinite vertical cylinder, **b** a horizontal cylinder and **c** a sphere as obtained from Eq. (1)

1.8 First real case: the Louga gravity anomaly

A residual gravity anomaly profile was collected from the west coast of Senegal (Nettleton, 1976). Figure 4 shows the appropriate residual gravity anomaly profile, 25 km long, and digitized at interims of 0.88 km. For every N value, the offered inverse method was utilized to the digitized anomaly profile to detect the model parameters z, q and A using Eqs. (12), (7) and (2), respectively (Table 8). Utilizing the estimated model parameters at various N values, the μ-value of the contrast among the observed and the calculated gravity anomalies (Fig. 4) was assessed. This Figure exhibits that the shape of the subsurface structure looks like a sphere (q = 1.55) at a depth of 9.09 km. The shape and the depth of the ore body attained through the current method are consistent very well with those achieved by Nettleton (1976) and Asfahani and Tlas (2011) (Table 9).

Table 9 indicates that the gravity parameters obtained by the suggested approach are in acceptable concurrence with those reported in different studies. Overall, there is a realistic

Fig. 2 The residual self-potential anomalies of the buried structures representing by: **a** a semi-infinite vertical cylinder, **b** a horizontal cylinder and **c** a sphere as obtained from Eq. (1)

concurrence between all results, except the amplitude factor ($A = 11{,}472.89$ mGal$\times$km^2) value (Table 9). The difference in A value is due to a discrepancy in the units used for A, as these units rely upon the shape factor (q) of the body.

1.9 Second real case: the Malachite mine anomaly

Another self-potential profile was measured on the Malachite mine, Jefferson County, Colorado, USA collected by Heiland et al. (1945) (Fig. 5). These measurements were analyzed and described by Dobrin (1960). A sulphide ore body was found almost in vertical—cylindrical massive shaped with 11 m width and 13.7 m depth (drilling information; Heiland et al. 1945; Dobrin 1960). Moreover, the sulphide mine was an amphibolite belt constrained by a schist and gneiss. A quartz diorite sheet was sliced through schists with about vertical dip and with lenticular copper sulfides. The self-potential investigation helped in assessing the potential

Table 5 Numerical results of the present method applied to synthetic example; the self-potential anomaly profile over a thin sheet model (q=0.5) with model parameters are z=2 unit, θ=30°, A=-500 mV, and profile length=40 unit without and with a 10% random noise

Synthetic data without random noise

N (unit)	z (unit)	e (%)	θ (deg.)	e (%)	q (dimensionless)	e (%)	A (mV)	e (%)	μ-value (mV)
2	2	0	30	0	0.5	0	− 500	0	0
3	2	0	30	0	0.5	0	− 500	0	0
4	2	0	30	0	0.5	0	− 500	0	0
5	2	0	30	0	0.5	0	− 500	0	0
6	2	0	30	0	0.5	0	− 500	0	0
7	2	0	30	0	0.5	0	− 500	0	0
8	2	0	30	0	0.5	0	− 500	0	0
9	2	0	30	0	0.5	0	− 500	0	0
10	2	0	30	0	0.5	0	− 500	0	0

Synthetic data with a 10% random noise

N (unit)	z (unit)	e (%)	θ (deg.)	e (%)	q (dimensionless)	e (%)	A (mV)	e (%)	μ-value (mV)
2	1.82	9.00	30.31	1.03	0.53	6.80	− 499.60	0.08	13.15
3	2.08	4.00	28.98	3.40	0.52	3.37	− 496.75	0.65	10.78
4	2.16	8.00	29.16	2.80	0.51	2.01	− 493.99	1.20	12.37
5	1.83	8.50	30.48	1.60	0.54	9.00	− 497.06	0.59	12.59
6	2.03	1.50	28.77	4.10	0.49	0.66	− 500.18	0.04	11.37
7	2.02	1.00	28.69	4.36	0.52	4.72	− 501.37	0.27	11.91
8	2.14	7.00	29.43	1.90	0.48	3.00	− 489.97	2.01	14.08
9	2.08	4.00	29.03	3.23	0.49	1.62	− 496.07	0.78	10.78
10	2.15	7.50	29.77	0.77	0.47	5.34	− 484.87	3.03	17.98

difference between equidistant points along with profile lines vertical to the extension of the ore body.

This anomaly profile was digitized at an interim of 6.8 m. All digitized self-potential values were used to calculate the model parameters z, θ, q, and A applying Eqs. (12), (8), (7) and (2) for each N value, respectively (Table 10). The detected parameters were applied to decide the optimal fit of the geometric body (shape factor) by utilizing the μ-value standard. The model with a minimum μ-value (8.338 mV) was for a 3D semi-infinite vertical cylinder model. Its parameters were: z=15.5 m, θ=79.2°, q=0.55, and A=− 240.4 mV (Fig. 5). The shape and the other model parameters recovered by our inversion method are in a good agreement with those attained by drilling information and with the outcomes available in other scientific literature such as Abdelrahman et al. (2004) and Tlas and Asfahani (2007) (Table 11).

Table 6 Numerical results of the present method applied to synthetic example; the self-potential anomaly profile over a horizontal cylinder model (q=1.0) with model parameters are z=4 unit, θ=50°, A=-2000 mV×unit, and profile length=40 unit, without and with a 10% random noise

Synthetic data without random noise

N (unit)	z (unit)	e (%)	θ (deg.)	e (%)	q (dimensionless)	e (%)	A (mV×unit)	e (%)	μ-value (mV)
2	4	0	50	0	1	0	− 2000	0	0
3	4	0	50	0	1	0	− 2000	0	0
4	4	0	50	0	1	0	− 2000	0	0
5	4	0	50	0	1	0	− 2000	0	0
6	4	0	50	0	1	0	− 2000	0	0
7	4	0	50	0	1	0	− 2000	0	0
8	4	0	50	0	1	0	− 2000	0	0
9	4	0	50	0	1	0	− 2000	0	0
10	4	0	50	0	1	0	− 2000	0	0

Synthetic data with a 10% random noise

N (unit)	z (unit)	e (%)	θ (deg.)	e (%)	q (dimensionless)	e (%)	A (mV×unit)	e (%)	μ-value (mV)
2	4.00	0	52.99	5.98	1.07	7.44	− 1993.62	0.32	10.87
3	3.87	3.25	51.48	2.96	0.96	4.02	− 1970.43	1.48	6.63
4	3.86	3.50	51.65	3.30	0.99	1.22	− 1961.31	1.93	6.86
5	3.85	3.75	50.71	1.42	0.97	3.19	− 1977.90	1.10	6.35
6	3.84	4.00	51.55	3.10	0.97	2.86	− 1951.01	2.45	6.77
7	3.89	2.75	49.61	0.78	0.95	5.32	− 2031.97	1.60	8.96
8	3.85	3.75	50.75	1.50	1.00	0.30	− 1980.98	0.95	6.34
9	3.86	3.50	50.71	1.42	1.06	6.04	− 1984.60	0.77	6.38
10	3.85	3.75	50.98	1.96	0.98	2.47	− 1970.04	1.50	6.26

2 Conclusions

This study proposed nonlinear least-squares method to detect the depth of a subsurface structure and calculate the model parameters for simple-class geometrical shapes bodies: spherical, horizontally and vertically cylindrical, to interpret gravity and/or self-potential combined formula. The procedure of the offered method mainly relied upon deciphering a non-linear equation z=f(z) and the statistical μ-value criteria between observed and computed anomalies and determine a preferable structure for the gravity and/or self-potential anomaly. The efficiency and sensitivity of the proposed method were investigated through analyzing and interpreting synthetic theoretical examples. Furthermore, the advantage of

Table 7 Numerical results of the present method applied to synthetic example; the self-potential anomaly profile over a sphere model (q = 1.5) with model parameters are z = 6 unit, θ = 70°, A = -35,000 mV × unit^2 and profile length = 40 unit, without and with a 10% random noise

Synthetic data without random noise

N (unit)	z (unit)	e (%)	θ (deg.)	e (%)	q (dimensionless)	e (%)	A (mV × unit^2)	e (%)	μ-value (mV)
2	6	0	70	0	1.5	0	− 3500	0	0
3	6	0	70	0	1.5	0	− 3500	0	0
4	6	0	70	0	1.5	0	− 3500	0	0
5	6	0	70	0	1.5	0	− 3500	0	0
6	6	0	70	0	1.5	0	− 3500	0	0
7	6	0	70	0	1.5	0	− 3500	0	0
8	6	0	70	0	1.5	0	− 3500	0	0
9	6	0	70	0	1.5	0	− 3500	0	0
10	6	0	70	0	1.5	0	− 3500	0	0

Synthetic data with a 10% random noise

N (unit)	z (unit)	e (%)	θ (deg.)	e (%)	q (dimensionless)	e (%)	A (mV × unit^2)	e (%)	μ-value (mV)
2	6.01	0.17	67.93	2.96	1.51	0.67	− 3488.09	0.34	13.90
3	6.21	3.50	69.59	0.58	1.48	1.33	− 3559.16	1.69	8.14
4	6.28	4.67	70.78	1.12	1.49	0.67	− 3572.60	2.07	12.03
5	6.16	2.67	68.71	1.84	1.52	1.33	− 3553.16	1.52	9.49
6	6.18	3.00	68.97	1.47	1.47	2.00	− 3558.99	1.69	8.70
7	6.19	3.17	69.97	0.04	1.49	0.67	− 3542.52	1.21	8.78
8	6.20	3.33	68.77	1.75	1.51	0.67	− 3574.85	2.14	9.25
9	6.19	3.17	69.47	0.76	1.50	0.00	− 3553.26	1.52	8.09
10	6.21	3.48	68.98	1.46	1.51	0.67	− 3575.58	2.16	8.68

using the proposed method over the earlier one is not need to priori information about the shape of the subsurface structure. The synthetic data revealed that the viability of the offered method was precise and firm. In addition, utilizing the proposed method to real data from Senegal and USA established that the acquired outcomes were reliable with the information from drilling and outcomes available in other works. Furthermore, the proposed method proved robust as it could be simply placed in a code. Besides, its convergence to the optimum model solutions was definite and rapid. Accordingly, this method is endorsed for routine exploration of field anomalies in an attempt to detect the geophysical parameters for the mentioned structures.
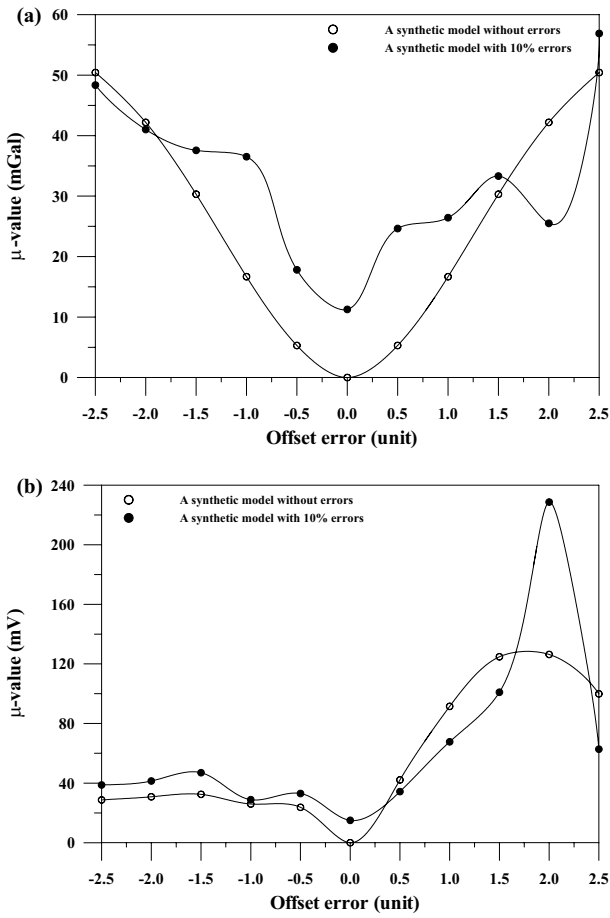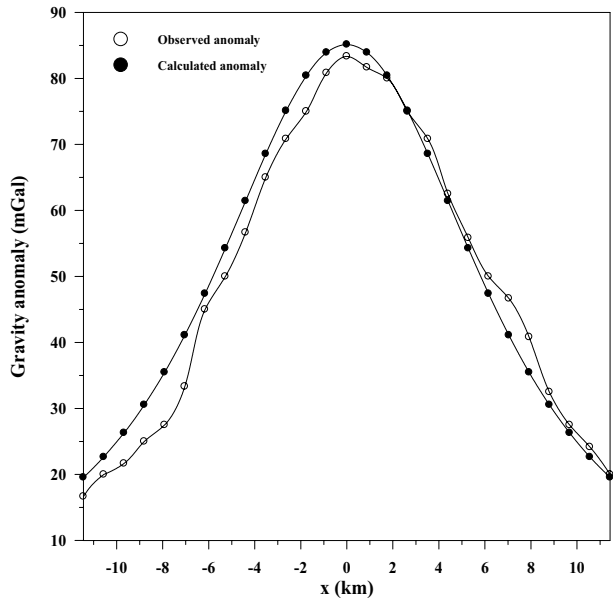
Fig. 3 The relation between offset and μ-value errors; **a** gravity model and **b** self-potential model

Fig. 4 The measured gravity anomaly (open circles) over an area on the west coast of Senegal and the calculated response (solid circles) computed from the present inverse algorithm
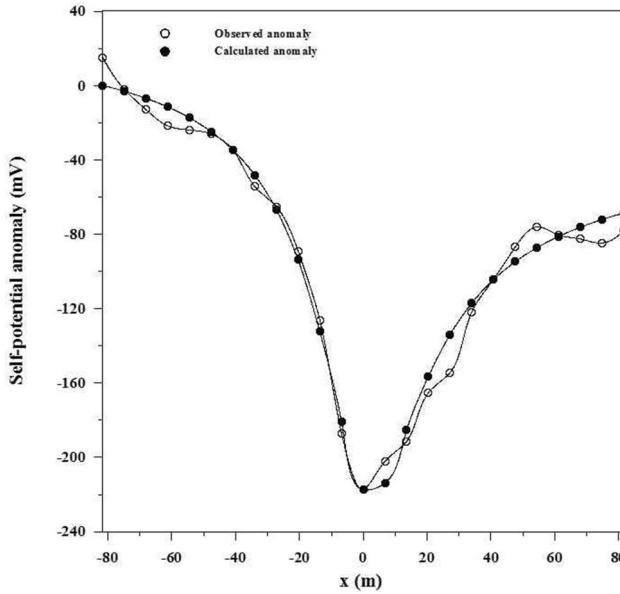

Table 8 Modeling results of the buried body of the Louga gravity anomaly, Senegal using the proposed method

N (km)	z (km)	q (dimensionless)	A (mGal×km²)	μ-value (mGal)
7.04	10.284	1.910	85,408.740	3.531
7.92	9.899	1.802	45,526.370	3.526
8.80	10.053	1.871	66,145.670	3.550
9.68	10.196	1.900	79,413.500	3.538
10.56	9.090	1.555	11,472.890	3.522
11.44	9.739	1.746	33,380.730	3.523

Table 9 Comparative results for the Louga gravity anomaly, Senegal

	Nettleton method (1976)	Asfahani and Tlas method (2011)	Suggested method
z (km)	9.30	9.13	9.09
q (dimensionless)	1.5 Assumed	1.499 estimated	1.55 estimated
A (mGal×km²)	–	6931.78	11,472.89

Fig. 5 The measured self-potential anomaly (open circles) over the Malachite mine, Jefferson County, Colorado, USA and the calculated response (solid circles) computed from the present inverse algorithm

Table 10 Modeling results of the buried body of the Malachite Mine self-potential anomaly, USA using the proposed method

N (m)	z (m)	q (dimensionless)	θ (deg.)	A (mV)	μ-value (mV)
34.00	16.067	0.531	79.716	− 233.196	8.470
40.80	15.498	0.550	79.214	− 240.382	8.338
47.60	16.676	0.609	79.285	− 268.797	10.783
54.40	17.674	0.626	80.347	− 280.337	12.693
61.20	15.334	0.512	81.776	− 223.923	10.804
68.00	14.387	0.481	81.220	− 213.663	9.067
74.80	13.780	0.471	80.041	− 211.856	8.971
81.60	15.176	0.568	74.553	− 251.619	14.735

Table 11 Comparative results for the Malachite Mine self-potential anomaly, USA

	Drilling information	Abdelrahman et al. method (2004)	Tlas and Asfahani method (2007)	Suggested method
z (m)	13.7	15.5	12.79	15.49
q (dimensionless)	–	0.5 assumed	0.5 assumed	0.55 estimated
θ (deg.)	–	83.4	79.98	79.2
A (mV)	–	− 227	− 229.28	− 240.3

References

Abdelrahman EM, El-Araby TM, Essa KS (2009) Shape and depth determinations from second moving average residual self-potential anomalies. J Geophys Eng 6:43–52

Abdelrahman EM, Essa KS, Abo-Ezz ER, Sultan M, Sauck WA, Gharieb AG (2008) New least-squares algorithm for model parameters estimation using self-potential anomalies. Comput Geosci 34:1569–1576

Abdelrahman EM, Essa KS, Abo-Ezz ER, Soliman KS (2006a) Self-potential data interpretation using standard deviations of depths computed from moving-average residual anomalies. Geophys Prospect 54:409–423

Abdelrahman EM, Essa KS, Abo-Ezz ER, Soliman KS, El-Araby TM (2006b) A least-squares depth-horizontal position curves method to interpret residual SP anomaly profiles. J Geophys Eng 3:252–259

Abdelrahman EM, El-Araby HM, Hassaneen AG, Hafez MA (2003) New methods for shape and depth determinations from SP data. Geophysics 68:1202–1210

Abdelrahman EM, Saber HS, Essa KS, Fouda MA (2004) A least-squares approach to depth determination from numerical horizontal self-potential gradients. Pure Appl Geophys 161:399–411

Aboud E, Salem A, Elawadi E, Ushijima K (2004) Estimation of shape factor of buried structure from residual gravity data. The 7th SEGJ International Symposium, November 24–26, 2004. Tohoku University, Sendai

Al-Garni MA (2008) Walsh transforms for depth determination of a finite vertical cylinder from its residual gravity anomaly. Sageep 6–10:689–702

Al-Garni MA (2010) Interpretation of spontaneous potential anomalies from some simple geometrically shaped bodies using neural network inversion. Acta Geophys 58:143–162

Asfahani J, Tlas M (2011) Fair function minimization for direct interpretation of residual gravity anomaly profiles due to spheres and cylinders. Pure Appl Geophys 168:861–870

Asfahani J, Tlas M, Hammadi M (2001) Fourier analysis for quantitative interpretation of Self-potential anomalies caused by horizontal cylinder and sphere. J Kau Earth Sci 13:41–54

Babu LA, Reddy KG, Mohan NL (1991) Gravity interpretation of vertical line element and slap–a Mellin transform method. Indian J Pure Appl Math 22:439–447

Bhattacharya BB, Roy N (1981) A note on the use of nomograms for self-potential anomalies. Geophys Prospect 29:102–107

Biswas A (2016a) Interpretation of gravity and magnetic anomaly over thin sheet-type structure using very fast simulated annealing global optimization technique. Model Earth Syst Environ 2:30

Biswas A (2016b) A comparative performance of least-square method and very fast simulated annealing global optimization method for interpretation of self-potential anomaly over 2-D inclined sheet type structure. J Geol Soc India 88:493–502

Biswas A, Sharma SP (2017) Interpretation of self-potential anomaly over 2-D inclined thick sheet structures and analysis of uncertainty using very fast simulated annealing global optimization. Acta Geod Geophys 52:439–455

Bowin C, Scheer E, Smith W (1986) Depth estimates from ratios of gravity, geoid, and gravity gradient anomalies. Geophysics 51:123–136

Chai T, Draxler RR (2014) Root mean square error (RMSE) or mean absolute error (MAE)? arguments against avoiding RMSE in the literature. Geosci Model Dev 7:1247–1250

Di Maio R, Rani P, Piegari E, Milano L (2016) Self-potential data inversion through a genetic-price algorithm. Comput Geosci 94:86–95

Dobrin MB (1960) Introduction to geophysical prospecting. Mc Graw Hil Book Company Inc, New York

El-Araby H (2004) A new method for complete quantitative interpretation of self-potential anomalies. J Appl Geophys 55:211–224

Essa KS (2007a) A simple formula for shape and depth determination from residual gravity anomalies. Acta Geophys 55:182–190

Essa KS (2007b) Gravity data interpretation using the s-curves method. J Geophys Eng 4:204–213

Essa KS (2010) A generalized algorithm for gravity or self-potential data inversion with application to mineral exploration. ASEG Ext Abstr 1:1–4

Essa KS (2011) A new algorithm for gravity or self-potential data interpretation. J Geophys Eng 8:434–446

Essa KS (2020) Self potential data interpretation utilizing the particle swarm method for the finite 2D inclined dike: mineralized zones delineation. ACTA Geod Geophys 55:203–221

Essa KS, Elhussein M (2017) A new approach for the interpretation of self-potential data by 2-D inclined plate. J Appl Geophys 136:455–461

Essa K, Mehanee S, Smith PD (2008) A new inversion algorithm for estimating the best fitting parameters of some geometrically simple body from measured self-potential anomalies. Explor Geophys 39:155–163

Essa KS, Munschy M (2019) Gravity data interpretation using the particle swarm optimization method with application to mineral exploration. J Earth Syst Sci 128:123

Ghanati R, Ghari H, Fatehi M (2017) Regularized nonlinear inversion of magnetic anomalies of simple geometric models using Occam's method: an application to the Morvarid iron-apatite deposit in Iran. ACTA Geod Geophys 52:555–580

Gupta OP (1983) A least-squares approach to depth determination from gravity data. Geophysics 48:537–360

Hajian A, Zomorrodian H, Styles P (2012) Simultaneous estimation of shape factor and depth of subsurface cavities from residual gravity anomalies using feed-forward back-propagation neural networks. ACTA Geophys 60:1043–1075

Hartmann RR, Teskey D, Friedberg I (1971) A system for rapid digital aeromagnetic interpretation. Geophysics 36:891–918

Heiland CA, Tripp MR, Wantland D (1945) Geophysical surveys at the Malachite Mine, Jefferson County, Colorado. Am Inst Min Metall Eng 164:142–154

Jain S (1976) An automatic method of direct interpretation of magnetic profiles. Geophysics 41:531–541

Mehanee SA, Essa KS (2015) 2.5D regularized inversion for the interpretation of residual gravity data by a dipping thin sheet: numerical examples and case studies with an insight on sensitivity and non-uniqueness. Earth Planets Space 67:130

Mohan NL, Anandababu L, Roa S (1986) Gravity interpretation using the Melin transform. Geophysics 51:114–122

Montesinos FG, Arnoso J, Vieira R (2005) Using a genetic algorithm for 3-D inversion of gravity data in Fuerteventura (Canary Islands). Int J Earth Sci (Geol Rundsch) 94:301–316

Murthy BVS, Haricharan P (1984) Self-potential anomaly over double line of poles—interpretation through log curves. Proc Indian ACAD Sci Earth Planet Sci 93:437–445

Mustoe LR, Barry MDJ (1998) Mathematics in engineering and science. Wiley, New York

Nandi BK, Shaw RK, Agarwal BNP (1997) A short note on identification of the shape of simple causative sources from gravity data. Geophys Prospect 45:513–520

Nettleton LL (1976) Gravity and magnetics in oil prospecting. McGraw-Hill Book Co, New York

Oksum E, Dolmaz MN, Pham LT (2019) Inverting gravity anomalies over the Burdur sedimentary basin, SW Turkey. ACTA GEOD GEOPHYS 54:445–460

Osman O, Muhittin AA, Ucan ON (2007) Forward modeling with Forced Neural Networks for gravity anomaly profile. MATH GEOL 39:593–605

Paul MK (1965) Direct interpretation of self-potential anomalies caused by inclined sheets of infinite horizontal extensions. Geophysics 30:418–423

Ram Babu HV, Atchuta Rao AD (1988) A rapid graphical method for the interpretation of the self-potential anomaly over a two-dimensional inclined sheet of finite depth extent. Geophysics 53:1126–1128

Reid AB, Allsop JM, Granser H, Millet AJ, Somerton IW (1990) Magnetic interpretation in three dimensions using Euler Deconvolution. Geophysics 55:80–91

Phama LT, Oksum E, Doa TD (2018) GCH_gravinv: A MATLAB-based program for inverting gravity anomalies over sedimentary basins. Comput Geosci 120:40–47

Roy L, Agarwal BNP, Shaw RK (2000) A new concept in Euler deconvolution of isolated gravity anomalies. Geophys Prospect 16:559–575

Roy IG (2019) On studying flow through a fracture using self-potential anomaly: application to shallow aquifer recharge at Vilarelho da Raia, northern Portugal. Acta Geod Geophys 54:225–242

Roy SVS, Mohan NL (1984) Spectral interpretation of self-potential anomalies of some simple geometric bodies. Pure Appl Geophys 78:66–77

Sharma B, Geldart LP (1968) Analysis of gravity anomalies of two-dimensional faults using Fourier transforms. Geophys Prospect 16:77–93

Shaw RK, Agarwal BNP, Nandi BK (1998) Walsh spectra of gravity anomalies over some simple sources. J Appl Geophys 40:179–186

Srivastava S, Datta D, Agarwal BNP, Mehta S (2014) Applications of ant colony optimization in determination of source parameters from total gradient of potential fields. Near Surf Geophys 12:373–390

Stanley JM (1977) Simplified magnetic interpretation of the geologic contact and thin dike. Geophysics 42:1236–1240

Sundararajan N, Srinivasa Rao P, Sunitha V (1998) An analytical method to interpret self-potential anomalies caused by 2D inclined sheets. Geophysics 63:1551–1555

Tarantola A (2005) Inverse problem theory and methods for model parameter estimation. SIAM, Philadelphia

Thompson DT (1982) EULDPH-A new technique for making computer-assisted depth estimates from magnetic data. Geophysics 47:31–37

Tikhonov AN, Arsenin VY (1977) Solutions of Ill-posed problems. John Wiley and Sons, New York

Tlas M, Asfahani J (2007) A best-estimate approach for determining self-potential parameters related to simple geometric shaped structures. Pure Appl Geophys 164:2313–2328

Vasiljević I, Ignjatović S, Đurić D (2019) Simple 2D gravity–density inversion for the modeling of the basin basement: example from the Banat area, Serbia. Acta Geophys 67:1747–1758